An Inclusive Search for the Higgs Boson in the Four Lepton Final State

The Higgs boson is the last undiscovered particle of the Standard Model of Particle Physics (SM). A search for SM Higgs boson decays in the four lepton final state is conducted using the full dataset collected by the CDF-II detector, corresponding to 9.7 fb^{-1} of data of $p\bar{p}$ collisions collected at Fermilab's Tevatron accelerator. We reconstruct the three final states of four electrons ($4e$), four muons (4μ) and pairs of electrons and muons ($2e2\mu$) in the ranges $50\,\mathrm{GeV}/c^2$ to $600\,\mathrm{GeV}/c^2$ of the four lepton invariant mass and 0 GeV to 200 GeV of the missing transverse energy. Our search is optimized for Higgs boson decays to Z-boson pairs but is sensitive, due to the measurement of the missing transverse energy, to the W-boson pair and τ-lepton pair decay channels of a Higgs boson, which is produced in association with a Z boson. We expect contributions from non-resonant ZZ production and fakes of 10.5 ± 1.3 and 0.4 ± 0.2 events, respectively. In the data we observe 9 events, which is consistent with no events from Higgs boson decays, therefore we extract upper limits for the cross-section of Higgs particle production. Our most stringent limits above and below the threshold for on-shell production of ZZ are set at Higgs boson masses of $150\,\mathrm{GeV}/c^2$ and $200\,\mathrm{GeV}/c^2$ with observed cross-sections of above 9.5 and 7.2 times that of the SM ruled out at the 95% confidence level, respectively.

The vector gauge bosons mediating the weak force, the W and Z, are massive. Within the Standard Model of Particle Physics (SM) their masses arise through electroweak spontaneous symmetry breaking [1, 2, 3] (SSB) mediated by the Higgs mechanism [4, 5]. The Higgs mechanism is needed to maintain gauge invariance of the theory in the presence of massive vector gauge bosons by positing the presence of a scalar field and is also able to provide mass to the fundamental fermions through Yukawa couplings. Upon quantization it predicts the existence of an associated particle, the Higgs boson, The discovery of the Higgs boson would unambiguously confirm electroweak SSB within the SM.

In this Letter we report on the inclusive search for the Higgs boson via processes that yield either four electrons ($4e$), four muons (4μ) or two electrons and two muons ($2e2\mu$) in the final state using data of $p\bar{p}$ collisions at center of mass energy 1.96 TeV collected with the CDF II detector [6], corresponding to $9.7\,\mathrm{fb}^{-1}$ of integrated luminosity. We conduct a search using the measured four lepton invariant mass (m_{4l}) and missing transverse energy ($\not\!\!E_T$) spectrum [30].

Higgs boson decays to pairs of Z bosons ($H \rightarrow ZZ$) are the dominant contribution to our final state for most Higgs boson masses considered and owing to the narrowness of the Higgs boson mass peak in the m_{4l} spectrum offers the best search sensitivity. Along with ggH and VBF production our search for $H \rightarrow ZZ$ is sensitive to associated Higgs particle production processes. We are also sensitive to the Higgs particle decays to W boson pairs ($H \rightarrow WW$) and τ-lepton pairs ($H \rightarrow \tau\tau$), which in turn decay into muons and electrons, where the Higgs boson is produced in association with a Z boson that decays to charged leptons. Significant improvement in the sensitivity is gained through the measurement of $\not\!\!E_T$ because the Higgs boson decays to two final state charged leptons from W-boson pairs and tau-lepton pairs provide significant $\not\!\!E_T$ from neutrino production, whilst no intrinsic $\not\!\!E_T$ is produced in SM $ZZ \rightarrow 4l$ production.

The detection of four leptons offers one of the cleanest signatures available for analysis at a hadron collider due to the small probability of jets to produce fake lepton candidates thus the requirement of four isolated identified leptons renders background from ubiquitous multi-jet processes negligible. Our analysis implements a minimal set of criteria that ensure four well reconstructed leptons only requiring same flavor for lepton pairs. This is the first search of its type where the sensitivity to more than one Higgs boson decay channel is simultaneously exploited in the four-lepton final state.

The CDF II detector consists of a solenoidal spectrometer with a silicon tracker and an open cell drift-chamber (COT) surrounded by calorimeters and muon detectors [6]. The geometry is characterized using the azimuthal angle ϕ and the pseudorapidity $\eta \equiv ln[\tan(\theta/2)]$, where θ is the polar angle relative to the proton beam axis. Transverse energy, E_T, is defined to be $E \sin\theta$, where E is the energy of an electromagnetic (EM) and hadronic calorimeter energy cluster. Transverse momentum, p_T, is the track momentum component transverse to the beam line. The most precise tracking and calorimetry is available in the central region, ($|\eta| \leq 1.1$). There is additional but less precise detection in the forward region, ($1.2 \leq |\eta| \leq 2.0$). Calorimetry but not tracking extends out into the far forward regions ($2.0 \leq |\eta| \leq 2.8$).

We perform this search using events that are triggered and leptons reconstructed in the same way as it's done in the search for H$\rightarrow$WW$\rightarrow \ell\nu\ell\nu$ at CDF[7].

This analysis uses physics objects identified as electron and muon candidates, which are referred to as electrons and muons for simplicity. In general electrons are detected by matching a central or forward track to energy deposited in the calorimeter while muons are detected by matching a central or forward track to the lack of a calorimeter deposit,

with or without associated stubs in the various muon chambers beyond the calorimeters. Taus are considered too difficult to detect to include in this search, except indirectly as they decay to electrons or muons in flight.

Candidate leptons are separated into eleven categories: three for electrons; seven for muons; and one for isolated tracks that project to detector regions with insufficient calorimeter coverage for energy measurements. The electron categories are distinguished by whether the electron is found in the central region, either a tight central electron or likelihood-based electron, or in the forward calorimeter ($|\eta| > 1.1$) where silicon-only tracking is available. Likelihood-based electrons selection is based on track quality, track-calorimeter matching, calorimeter energy, calorimeter profile shape, and isolation information. Five of the muon catecories rely on direct detection in the muon chambers that are distinguished by their acceptance in pseudorapidity: central muon detectors ($|\eta| < 0.65$), central muon extension detectors ($0.65 < |\eta| < 1.0$), and intermediate muon detector ($1.0 < |\eta| < 1.5$). The remaining two categories rely on track matches to minimum ionization deposits in the central and forward electromagnetic calorimeters respectively, and have no associated stubs in the fore-mentioned muon sub-detectors. All leptons are required to be isolated by imposing the condition that the sum of the transverse energy of the calorimeter towers in a cone of $\Delta R = \sqrt{(\Delta\phi)^2 + (\Delta\eta)^2}$ equal to 0.4 around the lepton be less than 10% of the electron E_T (muon p_T).

The probability that a jet will be misidentified as a lepton is measured using samples of jet data collected using four dfferent jet E_T trigger thresholds (20, 50 , 70 and 100 GeV) and corrected for the contributions of leptons from W and Z boson decays. The range of measured fake rates for the lepton categories, which vary according to E_T or p_T are: $0.5\% - 3\%$ central electrons, $2\% - 6\%$ forward electrons, $0.5\% - 4\%$ central muons, $0.5\% - 2\%$ extension muons, $0.5\% - 2\%$ intermediate muons, $0.5\% - 6\%$ COT track muons and $0.5\% - 3\%$ isolated tracks.

Each of the events analyzed is selected by a trigger, which performs real time selection of high-E_T electrons or high-p_T muons. One electron trigger requires an EM energy cluster in the central calorimeter with transverse energy greater than 18 GeV pointed to by a COT track with transverse momentum greater than 8 GeV. Muon triggers are based on track segments in the muon chambers that are matched to a COT track with transverse momentum greater than 18 GeV. Trigger efficiencies are measured using samples of observed leptonic Z decays [6]. The lepton matched to the trigger lepton must have transverse energy (momemtum) greater than 20 GeV for electrons (muons).

Additional charged leptons are required to have transverse energy (momentum) greater than 10 GeV. We require exactly four leptons, where each must be separated from any other by a minimum ΔR of 0.1. This analysis evolved from the CDF measurement of the ZZ production cross-section in the four lepton final state, where constraints on the invariant mass of opposite sign same flavor dilepton pairs are imposed in order to explicitly reconstruct Z bosons [8]. For Higgs boson masses less than $180\,\mathrm{GeV}/c^2$ one of the Z bosons is guaranteed to be off-shell, as such requirements on the mass become inefficient. Nominally the mass constraints for dilepton pairs masses are above $20\,\mathrm{GeV}/c^2$ and below $140\,\mathrm{GeV}/c^2$. In the all same flavor final state opposite charge pairings are assigned on the basis of the separation from the Particle Data Group mass for the Z-boson. Given the smallness of backgrounds we found having no explicit constraint on the mass improves our sensitivity to $H \to ZZ$. The Higgs boson signature can also involve jets of hadrons produced from the decay of one of associated vector boson in the ZH or WH process, forward quarks in the VBF process, or from the radiation of gluons. We place no restriction on the number of jets allowed in the event.

The selected events consist primarily of the background from non-resonant diboson production of $Z^{(*)}$-boson pairs (ZZ). To a much smaller extent we suffer from mis-reconstructed ZZ events and from $Z\gamma$ production in association with jets, both of which contribute with signatures of three or two real leptons with one or two fake leptons from jets and/or the photon. The background from top-pair production is found to be negligible.

The acceptances, efficiencies and kinematic properties of the signal and background processes are determined primarily using simulation. Events are simulated with PYTHIA[9] for processes involving Higgs boson production $gg/\mathrm{VBF} \to H \to Z^{(*)}Z^{(*)}$, associated production $(W/Z)H \to (W/Z)Z^{(*)}Z^{(*)}$, $ZH \to ZWW$, $ZH \to Z\tau\tau$ and non-resonant diboson ZZ production. A $Z\gamma$ sample is simulated according to the process described by Baur[10]. CTEQ5L parton distribution functions (PDFs) are used to model the momentum distribution of the initial-state partons [11].

The cross sections for each process are normalized to: next-to-next leading order (NNLO) calculations with logarithmic resummation (ggH [12, 13]), NNLO (VH [14, 15, 16]), and next-to-leading order calculations (VBF [14, 17], ZZ [18], and $Z\gamma$ [19]).

The response of the CDF II detector is modelled with a GEANT-based simulation [20]. Efficiency corrections for the simulated CDF II detector response for leptons and photon conversions are determined using samples of observed $Z \to ll$ and photon conversions respectively. A correction to the simulated track resolution is applied, which is obtained from a fit to the dimuon invariant mass in the Z peak.

To estimate the total contribution from fakes in data we reconstruct events with two or three leptons and additional jets that are prone to fake leptons and weight these events with the measured jet to lepton fake rate probabilities. This method yields a very small number of events that pass the selection (as expected). We therefore model the distribution using a weighted sum of the distributions derived from the ZZ and $Z\gamma$ MC samples. The kinematic distribution of

TABLE I: The expected and observed limits of the Higgs boson production cross section normalised to the SM prediction for Higgs particle masses from 120 GeV to 300 GeV in steps of 10 GeV.

H→4ℓ	120	130	140	150	160	170	180	190	200	210	220	230	240	250	260	270	280	290	300
$-2\sigma/\sigma_{SM}$	29.1	15.1	9.2	7.9	12.2	17.9	13.1	5.9	6.0	7.9	9.6	10.3	11.6	12.7	14.0	15.2	16.0	18.3	20.0
$-1\sigma/\sigma_{SM}$	31.2	16.2	9.7	8.1	12.8	19.6	14.0	7.3	7.9	9.7	11.3	12.5	12.9	14.7	16.0	18.0	18.0	20.6	22.4
Median/$\sigma_{\mathbf{SM}}$	**38.0**	**18.3**	**11.7**	**9.4**	**16.0**	**25.1**	**18.51**	**9.8**	**10.6**	**12.9**	**15.7**	**16.6**	**18.9**	**20.5**	**21.1**	**23.2**	**23.5**	**28.0**	**30.5**
$+1\sigma/\sigma_{SM}$	49.2	25.6	16.2	13.0	22.0	34.2	26.2	12.9	14.7	19.2	22.5	22.9	25.5	29.2	30.4	32.0	33.0	37.6	42.2
$+2\sigma/\sigma_{SM}$	66.6	33.6	21.0	16.6	27.1	48.8	39.9	18.4	20.7	27.8	29.0	30.5	33.6	40.6	42.0	47.2	49.2	47.4	58.3
Observed/$\sigma_{\mathbf{SM}}$	**42.4**	**20.5**	**12.6**	**9.5**	**16.8**	**28.5**	**16.3**	**8.2**	**7.2**	**7.9**	**10.3**	**20.5**	**21.1**	**17.4**	**17.3**	**18.2**	**19.9**	**24.1**	**28.6**

the component of fakes from badly reconstructed ZZ is assumed to be the same as that of correctly reconstructed ZZ events. We apply the same procedure to the $Z\gamma$ MC sample to obtain the invariant mass distribution for the remaining background component. This is found to be well modeled by a Landau function. In summary the overall normalization of the estimated fake background is derived using the data-driven approach while the shape of the distribution is derived from MC. We found the $\not\!\!E_T$ distribution for fakes from $Z\gamma$ to be very similar to that of ZZ, therefore we use the latter to model the fakes $\not\!\!E_T$ distribution in data.

Based on the selection described above in the ranges of $50 < m_{4l}/(\mathrm{GeV}/c^2) < 600$ and $0 < \not\!\!E_T/\mathrm{GeV} < 200$ we expect 10.59 ± 1.34 ZZ and 0.39 ± 0.19 fake events. For a SM Higgs boson with a mass of 150 GeV we expect conributions of: 0.23 (ggH), 0.02 (VBF), 0.01 (WH), and 0.15 (ZH) yielding a total of 0.41 ± 0.03 events. The indicated uncertainties are statistical and systematic, which are combined in quadrature. The latter are described below.

In data we observe a total of 9 events, which is consistent with no excess that could be assigned to Higgs Boson decays. The projections of four lepton invariant mass and $\not\!\!E_T$ distributions are plotted in Figure 1(a) and Figure 1(b) respectively, both overlayed with expected contributions from background and the Higgs boson production contribution for a mass of $150\,\mathrm{GeV}/c^2$. We consider only three $\not\!\!E_T$ bins that are defined by bin edges, $0-15-45-200$ GeV. The varied spacing was chosen as a compromise between discrimination of $ZH \to Z(WW/\tau\tau)$ from ZZ and stability for extracting a limit from the fit of the data. To cross check our result we examined the distribution in the number of jets, which was found to be consistent with that expected from ZZ production.

We set upper limits at the 95% confidence level (C.L.) on the Higgs boson production cross section, σ_H, expressed as a ratio to the expected SM rate as a function of m_H . We employ a Bayesian technique [21] using a likelihood function constructed from the joint Poisson probability of observing the data in each bin of the $m_{4l}-\not\!\!E_T$ phase space, integrating over the uncertainties of the normalization parameters using Gaussian priors. A constant prior in the signal rate is assumed. The expected limit and associated one and two sigma bands are given along with the observed limit in Table I and Fig. 2. We have comparable expected sensitivity at the intermediate mass (m_H =150 GeV/c^2) and at high mass (m_H =190 GeV/c^2), $9.4 \times \sigma_{SM}$ and $9.8 \times \sigma_{SM}$, at the 95% C.L. respectively, Our most stringent observed limits above and below the threshold for on-shell ZZ production are $9.5 \times \sigma_{SM}$ and $7.2 \times \sigma_{SM}$ at Higgs boson masses of 150 GeV/c^2 and 200 GeV/c^2, respectively, at the 95% C.L.[31]

When setting these limits we consider a variety of possible systematic effects including both those that change the normalization and the shape of the kinematic distributions. The dominant systematic uncertainties are those on the theory predictions for the cross sections of signal and background processes. Systematic uncertainties associated with the Monte Carlo simulation affect the Higgs particle production, ZZ and $Z\gamma$ acceptances taken from the simulated event samples.

Uncertainties originating from the lepton selection and trigger efficiency measurements are propagated through the acceptance calculation leading to uncertainies of 3.6% and 0.5%, respectively, on the predicted signal and background event yields. In addition, all signal and background estimates obtained from simulation have an additional 5.9% uncertainty originating from the measurement of the luminosity [22]. The $gg \to H$ cross-section has been computed at next-to-next leading order (NNLO) and next-to-next leading log (NNLL) precision with the associated scale and PDF α_s variations [23, 24, 25]. We apply a systematic uncertainty of 7% and 7.7% for the scale and PDF+α_s variations, respectively. Uncertainties from VBF and associated Higgs boson production channels, which account for about a quarter of the total Higgs boson production events are assigned uncertainties of 5% and 10%, respectively, according to the recommendation of the TeV4LHC working group [26]. A 3% uncertainty is assigned on the branching fraction of $H \to ZZ$ and $H \to WW$, which are 100% correlated, as well as a 3% uncertainty on $H \to \tau\tau$ [26]. The Pythia ZZ production Monte Carlo used for acceptances and efficiency determination is at LO; using MCFM[27] we

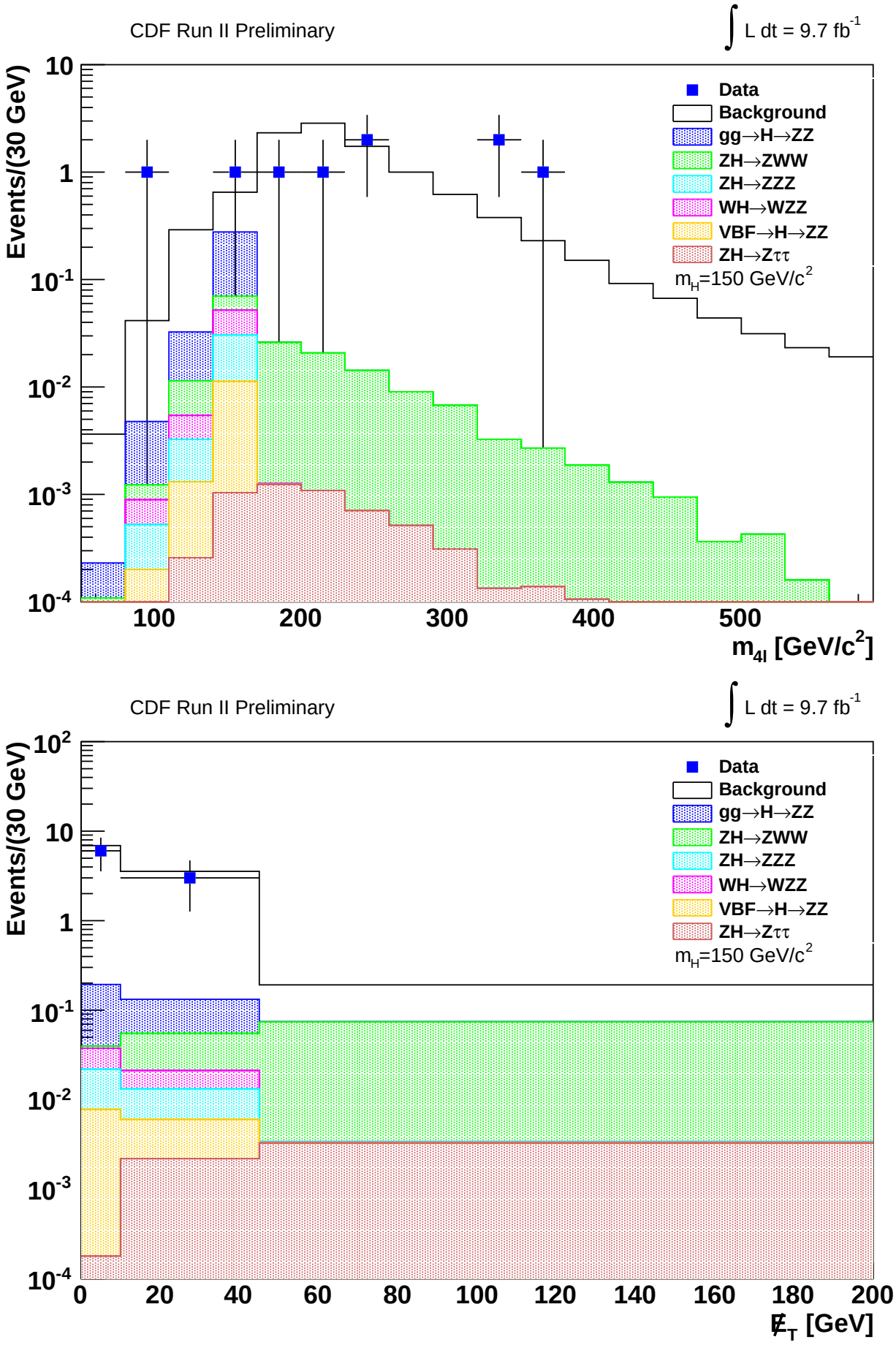

FIG. 1: The distributions of the four-lepton invariant mass (TOP) and the missing transverse energy (BOTTOM) as measured in data. Overlayed are estimated combined contributions from non-resonant ZZ production and fakes component, which are denoted as background. The contribution from Higgs boson decays are stacked and overlayed for a Higgs particle mass of 150 GeV/c^2.

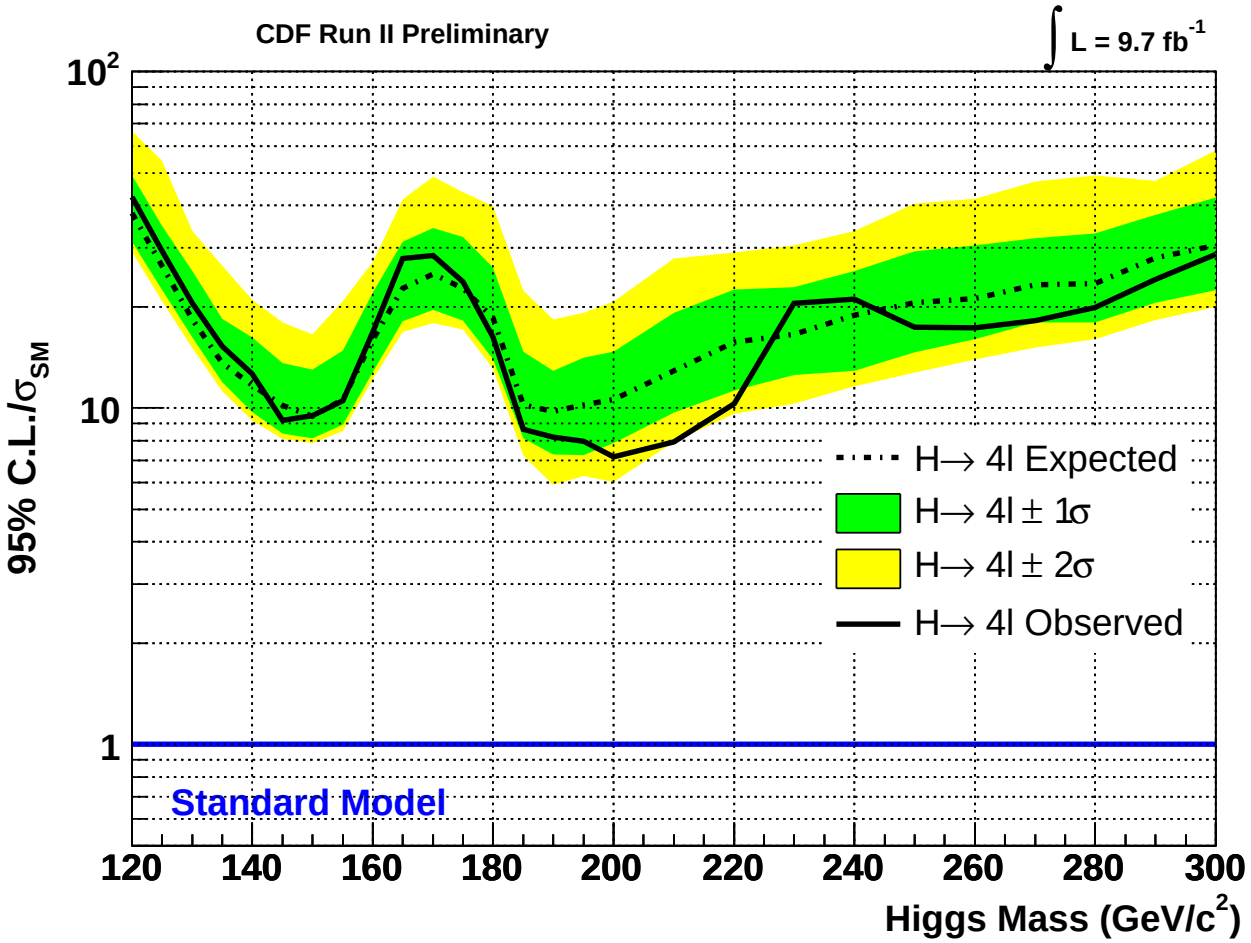

FIG. 2: The expected and observed limits of the Higgs boson production cross section normalised to the SM prediction as a function of the Higgs particle mass as derived from the search in the four lepton final state.

calculated the difference in the acceptance due to a full NLO simulation and found it to be $\pm 2.5\%$, which is assigned as a systematic uncertainty. We assign a 10% uncertainty on the ZZ cross-section based on the difference of predictions between LO and NLO [28]. For the Zγ spectrum in the four lepton invariant mass we assign an uncorrelated 50% uncertainty on the yield in each bin to account for potential mis-modelling from the use of the Landau function to model the shape. We measure the fake rates in several jet samples and we consider the maximum spread between these measurements as a systematic uncertainty on the background estimation. Propagated through to the acceptance this results in a 50% variation in the fakes yield. The $\not\!\!E_T$ is scaled up and down by 20% to account for potential MC mis-modelling, which is included as a shape systematic uncertainty in the limit calculation. A summary is given in Tab II.

In 9.7fb^{-1} of data we see no evidence, as expected, for a Higgs boson in the mass range $100\,\mathrm{GeV}/c^2$ to $300\,\mathrm{GeV}/c^2$. We set limits on the Higgs boson production cross section in the inclusive four lepton final state, exploiting the best current sensitivity not only in the high mass region where both Z's are produced on-shell but also in the lower mass region at the mass of around $150\,\mathrm{GeV}/c^2$ where additional signal contributions from $ZH \to ZWW$ and $ZH \to Z\tau\tau$ greatly improve the sensitivity.

We thank the Fermilab staff and the technical staffs of the participating institutions for their vital contributions. This work was supported by the U.S. Department of Energy and National Science Foundation; the Italian Istituto Nazionale di Fisica Nucleare; the Ministry of Education, Culture, Sports, Science and Technology of Japan; the Natural Sciences and Engineering Research Council of Canada; the National Science Council of the Republic of China; the Swiss National Science Foundation; the A.P. Sloan Foundation; the Bundesministerium für Bildung und Forschung, Germany; the Korean World Class University Program, the National Research Foundation of Korea; the Science and Technology Facilities Council and the Royal Society, UK; the Institut National de Physique Nucleaire et

TABLE II: Summary of the variations considered in the evaluation of systematic uncertainty on the limit extraction

Uncertainty Source	ZZ	$Z(\gamma^*)$	gg→H	WH	ZH	VBF
Cross Section						
Scale			7.0%			
PDF			7.7%			
Total	10%			5%	5%	10%
Branching Ratio			3%	3%	3%	3%
Acceptance						
Higher-order Diagrams	2.5%					
PDF	2.7%					
Luminosity	5.9%		5.9%	5.9%	5.9%	5.9%
Lepton ID Efficiencies	3.6%		3.6%	3.6%	3.6%	3.6%
Trigger Efficiencies	0.4%		0.5%	0.5%	0.5%	0.5%
Fake Rates		50%				
$\not\!\!E_T$			Shape uncertainty			

Physique des Particules/CNRS; the Russian Foundation for Basic Research; the Ministerio de Ciencia e Innovación, and Programa Consolider-Ingenio 2010, Spain; the Slovak R&D Agency; the Academy of Finland; and the Australian Research Council (ARC).

[1] Y. Nambu and G. Jona-Lasinio, Phys. Rev. **122**, 345 (1961).
[2] Y. Nambu and G. Jona-Lasinio, Phys. Rev. **124**, 246 (1961).
[3] Y. Nambu, Int. J. Mod. Phys. **A24**, 2371 (2009).
[4] P. W. Higgs, Phys. Lett. **12**, 132 (1964).
[5] P. W. Higgs, Phys. Rev. Lett. **13**, 508 (1964).
[6] A. Abulencia et al. (CDF Collaboration), J.Phys.G **G34**, 2457 (2007).
[7] T. Aaltonen et al. (CDF and D0), Phys. Rev. Lett. **104**, 061802 (2010).
[8] M. Bauce, *et al.* (CDF Collaboration) (2009), CDF/PHYS/ELECTROWEAK/PUB/9910.
[9] T. Sjostrand, S. Mrenna, and P. Skands, JHEP **05**, 026 (2006).
[10] U. Baur and E. L. Berger, Phys. Rev. **D47**, 4889 (1993).
[11] H. L. Lai *et al.* (CTEQ), Eur. Phys. J. **C12**, 375 (2000).
[12] D. de Florian and M. Grazzini, Phys. Lett. **B674**, 291 (2009).
[13] C. Anastasiou, R. Boughezal, and F. Petriello, JHEP **04**, 003 (2009).
[14] K. Assamagan et al. (Higgs Working Group Collaboration), pp. 1–169 (2004), hep-ph/0406152.
[15] O. Brein, A. Djouadi, and R. Harlander, Phys. Lett. **B579**, 149 (2004).
[16] M. L. Ciccolini, S. Dittmaier, and M. Kramer, Phys. Rev. **D68**, 073003 (2003).
[17] E. L. Berger and J. M. Campbell, Phys. Rev. **D70**, 073011 (2004).
[18] J. Campbell and R. K. Ellis, Phys. Rev. **D60**, 113006 (1999).
[19] U. Baur, T. Han, and J. Ohnemus, Phys. Rev. **D57**, 2823 (1998).
[20] R. Brun, R. Hagelberg, M. Hansroul, and J. Lassalle, CERN-DD-78-2-REV and CERN-DD-78-2.
[21] K. Nakamura et al. (Particle Data Group), J.Phys.G **G37**, 075021 (2010).
[22] D. Acosta *et al.*, Nucl. Instrum. Meth. **A494**, 57 (2002).
[23] M. Grazzini, *Hnnlo*, http://theory..infn.it/grazzini/codes.html.
[24] S. Catani and M. Grazzini, Phys.Rev.Lett. **98**, 222002 (2007).
[25] M. Grazzini, JHEP **0802**, 043 (2008).
[26] TeV4LHC, *Standard model higgs cross sections at hadron colliders*, http://maltoni.home.cern.ch/maltoni/TeV4LHC/SM.html.
[27] J. Campbell, K. Ellis, and C. Williams, *Monte carlo for femtobarn processes*, http://mcfm.fnal.gov/mcfm.pdf.
[28] J. M. Campbell and R. K. Ellis, Phys. Rev. **D60**, 113006 (1999).
[29] T. Aaltonen et al. (CDF), Phys. Rev. **D83**, 112008 (2011), 1102.4566.
[30] The missing transverse energy vector $\vec{\not\!\!E}_T$ is defined as the opposite of the vector sum of the E_T of all calorimetric towers, corrected to produce the correct average calorimeter response to jets and to muons.
[31] This result is consistent with the excess observed in the search for high-mass resonances decaying to ZZ [29] for a Higgs boson with a mass of about 325 GeV/c^2. This analysis is performed using CDF standard tracking algorithms while that uses an alternative reconstruction.